

# Quantum regulation of Ge nanodot state by controlling barrier of the interface layer

Yasuo Nakayama<sup>a)</sup>

CREST, Japan Science and Technology Agency, Saitama 332-0012, Japan

Iwao Matsuda and Shuji Hasegawa

Department of Physics, Graduate School of Science, The University of Tokyo, Tokyo 113-0033, Japan

Masakazu Ichikawa

CREST, Japan Science and Technology Agency and Quantum-Phase Electronics Center,  
Department of Applied Physics, Graduate School of Engineering, The University of Tokyo,  
Tokyo 113-8656, Japan

(Received 19 February 2006; accepted 23 May 2006; published online 20 June 2006)

Quantized energy in Ge nanodots aligned over oxidized Si surfaces could be regulated by modifying an interface atomic layer. The confining potential was evaluated from dot-size dependent energy shift of the ground state of confined holes, which revealed that epitaxial nanodots showed a lower confining potential barrier than nonepitaxial ones. The present results provide a new way to tune quantized energy levels of Ge nanodots not only by their size but also by interface condition. © 2006 American Institute of Physics. [DOI: 10.1063/1.2216893]

Quantum-size Ge nanostructures have been considered to be a promising material for Si-based optoelectronics devices.<sup>1-4</sup> The quantum confinement phenomena are induced at room temperature if the structure size is smaller than 10 nm.<sup>5,6</sup> However, well-used conventional process of self-organization has only enabled us to fabricate Ge clusters down to 30 nm in diameter.<sup>7,8</sup> In this context, Ge nanodots formed on an oxidized Si surface would be particularly promising owing to their sufficiently small size (smaller than 10 nm in diameter), size tunability, extremely high density (larger than  $10^{12}$  cm<sup>-2</sup>), as well as photoluminescence capability at RT.<sup>9-11</sup> A reflection-high-energy electron diffraction (RHEED) pattern of the Ge nanodots produced by this method at growth temperature of 350 °C shows Debye rings which are caused by the random orientation of Ge dots with respect to the Si substrate [Fig. 1(a)]. It means that the nanodots are separated from the Si substrate by the SiO<sub>2</sub> thin layer as sketched in Fig. 1(c). On the other hand, the Ge nanodots grown at 550 °C provide another RHEED pattern with diffuse spots, as shown in Fig. 1(b), indicating that the nanodots grow epitaxially to the Si(111) substrate. This is due to voids created in the SiO<sub>2</sub> layer, and the Ge nanodots can therefore align and grow epitaxially to the Si(111) through the voids [Fig. 1(d)].<sup>9</sup> Transmission electron microscopy (TEM) images also support the existence of voids through the SiO<sub>2</sub> film beneath the dot.<sup>12,13</sup>

We recently reported quantum confinement effect into the epitaxial Ge nanodots by means of photoemission spectroscopy (PES) and scanning tunneling microscopy (STM).<sup>14,15</sup> The obtained confinement potential barrier was significantly smaller than the value expected from the energy position of valence band maxima (VBM) of SiO<sub>2</sub> and bulk Ge. These facts imply that the potential barrier at the Ge/SiO<sub>2</sub>-Si interface is expected to be tunable by changing the growth temperature. The potential barrier height is thought to be an essential value correlating with the energy position of the quantized states<sup>14,16,17</sup> and also with electro-

luminescence efficiency via accessibility of the carriers into the nanodots.<sup>18</sup> In the present study, we have conducted PES and STM studies on the Ge nanodots formed under different growth conditions, which clearly indicates that the confining potential barrier height is regulated by the interface condition.

Ge nanodots on the ultrathin SiO<sub>2</sub> layer was prepared by the same procedure as reported before.<sup>9,14</sup> The Si substrates were cut from a mirror-polished *n*-type Si(111) wafer (1–10 Ω cm). A clean Si(111) 7×7 surface was primarily prepared by repeating cycles of resistive heating up to

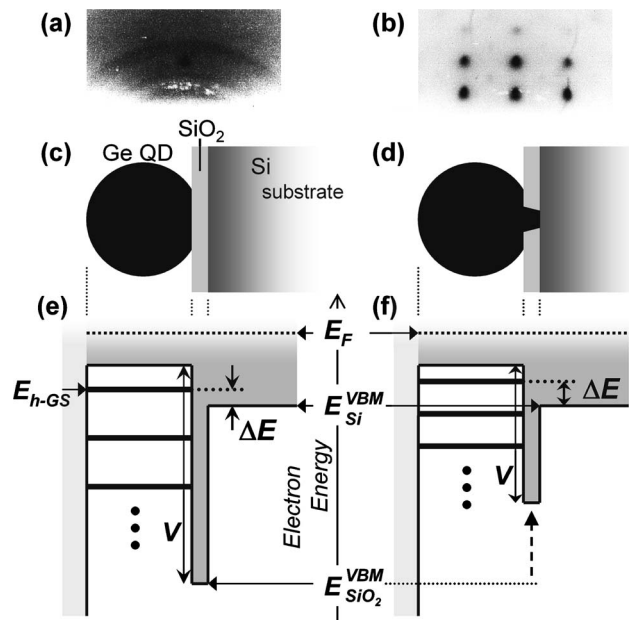


FIG. 1. [(a) and (b)] Typical RHEED patterns, [(c) and (d)] schematic drawings of the structures, and [(e) and (f)] the expected energy diagrams in valence band region of nonepitaxial [(a), (c), and (e)] and epitaxial Ge nanodots [(b), (d), and (f)], respectively. The Ge nanodots (black) are formed on a Si(111) substrate (dark gray) covered with an ultrathin SiO<sub>2</sub> (light gray).

<sup>a)</sup>Electronic mail: nakayama@surface.phys.s.u-tokyo.ac.jp

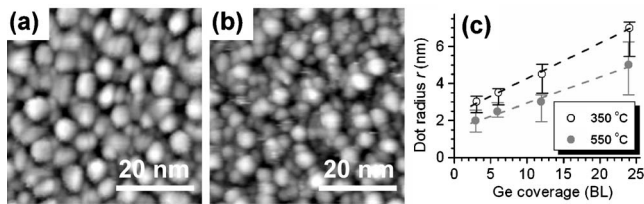


FIG. 2. Typical STM images of 3 BL-Ge nanodots formed at (a) 350 °C and (b) 550 °C. The images were taken in constant-current mode at  $V_{tip} = -3$  V and  $I_t = 0.24$  nA. (c) The dominant radius of Ge nanodots in which the largest population of deposited Ge belongs, plotted as a function of Ge coverage.

1200 °C in ultrahigh vacuum (UHV). Oxygen exposure ( $2 \times 10^{-4}$  Pa) onto the surface in increasing the sample temperature up to 630 °C generates a 0.3-nm-thick  $\text{SiO}_2$  layer over the Si(111).<sup>9</sup> Ge was deposited onto the ultrathin  $\text{SiO}_2$  layer from an alumina-coated tungsten basket. The evaporation rate of Ge was separately determined from a completion of  $5 \times 5$  RHEED pattern on the clean Si(111)  $7 \times 7$  kept at 610 °C [which was defined as 3 BL (bilayer)]<sup>18</sup>. 1 BL corresponds to  $1.57 \times 10^{15}$  cm<sup>-2</sup>, atom density in a double layer of Si(111) truncated surface.<sup>19</sup> PES measurements were carried out with He  $I\alpha$  radiation (21.22 eV) and a commercial electron spectrometer (VG, ADES 400). The  $E_F$  was determined from a tantalum clamp plate which was in good electrical contact with the sample. All spectra were taken at normal-emission angle. STM observation was performed at room temperature by a commercial STM apparatus with electrochemically polished W tips in another UHV chamber.

STM images of the Ge nanodots grown at different substrate temperatures are shown in Figs. 2(a) and 2(b). Typical size of the nanodots formed at 350 °C seems to be significantly larger than that at 550 °C even with the same deposited amount of Ge. This is because a portion of the deposited Ge is spent for creation of the voids on the  $\text{SiO}_2$  film through a certain deoxidization reaction at 550 °C.<sup>9</sup> Dot size was evaluated by counting data pixels for individual nanodots on the STM images, and through a statistical procedure conducted on these data of the dot size, we estimated the dominant size of the Ge nanodots at each Ge coverage in which the largest population of the deposited Ge is contained. The relationship between the Ge coverage and the dominant radius of the Ge nanodots is shown in Fig. 2(c). The error bars indicate the distribution in dot size. It is again shown that the dominant size of the Ge dots formed at 350 °C is significantly larger than that formed at 550 °C all through the coverage range. The former corresponds to the nonepitaxial nanodots, while the latter is epitaxial nanodots. The radius of the dots seems to grow almost linearly to the coverage in this range for both temperatures, which allows us to relate the coverage into the dot size.

Typical photoemission spectra from the same-sized Ge nanodots formed at 350 and 550 °C are shown in Fig. 3(a). Spectra from a bare  $\text{SiO}_2$  film is also shown for comparison. A large peak at binding energy ( $E_B$ ) of 6–8 eV is assigned to O  $2p$  states of the Si–O–Si bonds,<sup>20,21</sup> and the peak onset located at  $E_B = 4.5$ –5 eV corresponds to the VBM of the  $\text{SiO}_2$  film ( $E_{\text{SiO}_2}^{\text{VBM}}$ ). Since the mean free path of the present photoelectrons is about 1 nm, which is much longer than the thickness of the  $\text{SiO}_2$  layer (0.3 nm), spectral components between  $E_{\text{SiO}_2}^{\text{VBM}}$  and  $E_F$  can be attributed to bulk states from

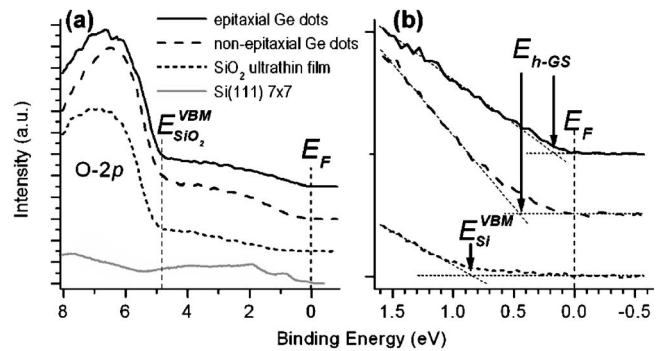


FIG. 3. (a) Photoemission spectra from the Ge nanodots formed on the ultrathin  $\text{SiO}_2$  layer at 550 °C (solid lines; epitaxial dots) and 350 °C (dashed lines; nonepitaxial dots). The dominant radius of the nanodots is commonly ca. 3.5 nm. Spectra from the bare  $\text{SiO}_2$  film and clean Si(111)  $7 \times 7$  are also presented as dotted lines and a gray solid line, respectively. (b) Magnified spectra near  $E_F$ .

the buried Si substrate. From the magnified spectra near  $E_F$  from the surface without Ge dots [dotted line in Fig. 3(b)], the threshold of the spectra around  $E_B = 0.9$  eV should be assigned to the VBM of the Si(111) substrate ( $E_{\text{Si}}^{\text{VBM}}$ ). By adding Ge nanodots, the spectral onset shifts closer to  $E_F$  than  $E_{\text{Si}}^{\text{VBM}}$ . The origin of such components can be ascribed to the electronic state in the Ge nanodots. This spectral onset corresponds to the highest occupied state (VBM of Ge nanodots), which is, in other words, the ground state of holes ( $h$ -GS) generated in the Ge nanodots by quantum confinement effect.<sup>14</sup> By following a method in Ref. 14, we estimate the energy position of VBM of the Ge dots as an intersection of two lines extrapolated from a spectral tail of the valence band of the Ge nanodots and background signals. Although such analysis cannot provide the absolute value of the binding energy of  $h$ -GS ( $E_{h\text{-GS}}$ ), it will allow us to trace the shift of  $E_{h\text{-GS}}$  [see Figs. 1(e) and 1(f) for the definitions of energy levels].

Figure 4 shows the energy shift of  $E_{h\text{-GS}}$  with respect to the VBM of Si substrate ( $E_{\text{Si}}^{\text{VBM}}$ ),  $\Delta E$  [see Fig. 1(e) for definition], plotted as a function of the dominant radius ( $r$ ) of the Ge nanodots.  $E_{h\text{-GS}}$  shifts away from  $E_{\text{Si}}^{\text{VBM}}$  as the nanodots grow. It should be also noted that the energy positions of

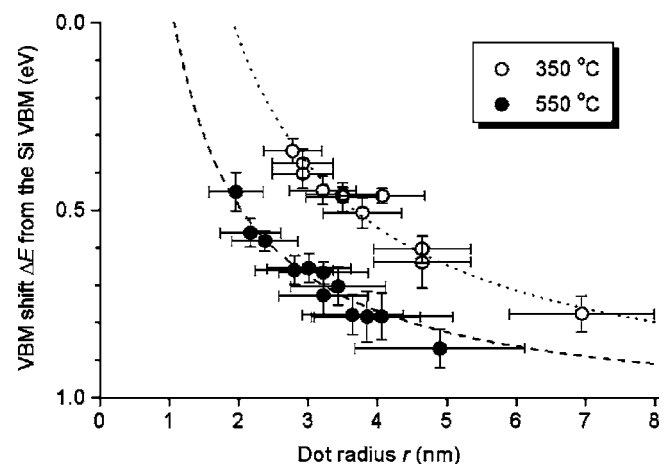


FIG. 4. Energy shift of the VBM  $\Delta E$  of nonpitaxial (350 °C) and epitaxial (550 °C) Ge nanodots plotted as a function of the dominant radius  $r$  of the nanodots. Least-squares fits by  $\Delta E \propto r^{-1}$  for the two data sets are drawn by dotted and dashed lines.

$E_{h\text{-GS}}$  are different depending on the growth temperature even at the same sizes of dots.

Energy level  $E_{h\text{-GS}}$  in a spherical quantum dots is analytically solvable by assuming a harmonic confining potential,<sup>14,16,17</sup>

$$E_{h\text{-GS}} = -V + 2a_B \sqrt{\frac{Ry}{m_h^*} \frac{\sqrt{V}}{r}} = E_0 - \Delta E, \quad (1)$$

where  $Ry$  is the atomic Rydberg and  $a_B$  is the atomic Bohr radius. We adopt the conductivity effective mass of holes as  $m_h^*$ .  $E_0$  is an energy reference and it is unnecessary to be determined in the present procedure, while a common value is adopted for  $E_0$  for both the epitaxial and nonepitaxial nanodots. Equation (1) means that the energy levels in the dots are governed by two physical properties, the confining potential barrier height  $V$  and the dot radius  $r$ .

We have demonstrated a least-squares fit of the experimental  $\Delta E$  with Eq. (1) for each growth temperature, as shown in Fig. 4. It gives the confining potential barrier height of 6.7 ( $\pm 0.9$ ) eV for the growth temperature of 350 °C and 2.1 ( $\pm 0.4$ ) eV for 550 °C. In the case of the nonepitaxial nanodots (grown at 350 °C), the obtained confining potential height is substantially larger than the potential barrier expected from the energy difference between the valence band maximum of bulk Ge (0.33 eV below  $E_F$ )<sup>22</sup> and  $E_{\text{SiO}_2}^{\text{VBM}}$  of the underlying ultrathin SiO<sub>2</sub> film [ca. 5 eV below  $E_F$ , see Fig. 3(a)]. We speculate that such an enlargement of the effective potential barrier is due to the fact that the major part of the surface area of the spherical nanodots is surrounded by vacuum and only a small area of the dot surface touches the oxidized Si surface. On the other hand, the confining potential for the epitaxial nanodots (grown at 550 °C) is significantly reduced compared to that of the nonepitaxial ones. This potential reduction should be attributed to the voids penetrating through the SiO<sub>2</sub> film. Thus the growth condition and resulting interface structure sensitively affect the quantum confinement in the nanodots.

The different barrier heights of confining potential cause the energy shifts of quantized states in the dots. Since the origin of the PL from Ge dots–SiO<sub>2</sub> systems has been assigned as the recombination between the confined holes in the Ge dots and electrons trapped at the defects on the adjoining SiO<sub>2</sub>,<sup>3,10,14</sup> our present results suggest a possibility for regulating the quantum-dot state through controlling the potential barrier height between the dots and substrate even if the dot size is unchanged.

In conclusion, we have carried out PES and STM studies on Ge nanodots formed at different growth temperatures and evaluated the confining potential barrier height for each temperature from the dot-size dependent shift of the energy position of the highest occupied quantum state. The confining potential is effectually reduced by the voids created at the ultrathin SiO<sub>2</sub> film between the dots and the substrate. The present results will provide an additional way for tuning the optoelectronic properties of the Ge nanodots.

This work was supported by the Core Research of Evolutional Science and Technology (CREST) of the Japan Science and Technology Agency (JST) and by the Japanese Society for the Promotion of Science (JSPS).

- <sup>1</sup>M. Zacharias and P. M. Fauchet, *Appl. Phys. Lett.* **71**, 380 (1997).
- <sup>2</sup>S. Takeoka, M. Fujii, S. Hayashi, and K. Yamamoto, *Phys. Rev. B* **58**, 7921 (1998).
- <sup>3</sup>Y. M. Niquet, G. Allan, C. Delerue, and M. Lannoo, *Appl. Phys. Lett.* **77**, 1182 (2000).
- <sup>4</sup>C. Bostedt, T. van Buuren, J. M. Plitzko, T. Möller, and L. J. Terminello, *J. Phys.: Condens. Matter* **15**, 1017 (2003).
- <sup>5</sup>A. I. Yakimov, V. A. Markov, A. V. Dvurechenskii, and O. P. Pchelyakov, *J. Phys.: Condens. Matter* **6**, 2573 (1994).
- <sup>6</sup>E. Leobandung, L. Guo, Y. Wang, and S. Y. Chou, *Appl. Phys. Lett.* **67**, 938 (1995).
- <sup>7</sup>Y.-W. Mo, D. E. Savage, B. S. Swartzentruber, and M. G. Lagally, *Phys. Rev. Lett.* **65**, 1020 (1990).
- <sup>8</sup>A. A. Shklyae, M. Shibata, and M. Ichikawa, *Phys. Rev. B* **58**, 15647 (1998).
- <sup>9</sup>A. A. Shklyae, M. Shibata, and M. Ichikawa, *Phys. Rev. B* **62**, 1540 (2000).
- <sup>10</sup>A. A. Shklyae and M. Ichikawa, *Appl. Phys. Lett.* **80**, 1432 (2002).
- <sup>11</sup>A. A. Shklyae and M. Ichikawa, *Surf. Sci.* **514**, 19 (2002).
- <sup>12</sup>A. V. Kolobov, A. A. Shklyae, H. Oyanagi, P. Fons, S. Yamasaki, and M. Ichikawa, *Appl. Phys. Lett.* **78**, 2563 (2001).
- <sup>13</sup>S. P. Cho, N. Tanaka, and M. Ichikawa (unpublished).
- <sup>14</sup>A. Konchenko, Y. Nakayama, I. Matsuda, S. Hasegawa, Y. Nakamura, and M. Ichikawa, *Phys. Rev. B* **73**, 113311 (2006).
- <sup>15</sup>Y. Nakamura, K. Watanabe, Y. Fukuzawa, and M. Ichikawa, *Appl. Phys. Lett.* **87**, 133119 (2005).
- <sup>16</sup>J. Adamowski, M. Sobkowicz, B. Szafran, and S. Bednarek, *Phys. Rev. B* **62**, 4234 (2000).
- <sup>17</sup>M. Ciurla, J. Adamowski, B. Szafran, and S. Bednarek, *Physica E (Amsterdam)* **15**, 261 (2002).
- <sup>18</sup>Y. Nakamura, Y. Nagadomi, K. Sugie, N. Miyata, and M. Ichikawa, *J. Appl. Phys.* **95**, 5014 (2004).
- <sup>19</sup>Y. Kajiyama, Y. Tanishiro, and K. Takayanagi, *Surf. Sci.* **222**, 47 (1989).
- <sup>20</sup>K. Sakamoto, S. Doi, Y. Ushimi, K. Ohno, H. W. Yeom, T. Ohta, S. Suto, and W. Uchida, *Phys. Rev. B* **60**, R8465 (1999).
- <sup>21</sup>J. W. Keister, J. E. Rowe, J. J. Kolodziej, H. Niimi, T. E. Madey, and G. Lucovsky, *J. Vac. Sci. Technol. B* **17**, 1831 (1999).
- <sup>22</sup>S. M. Sze, *Physics of Semiconductor Devices*, 2nd ed. (Wiley, New York, 1986).